Annals of Glaciology 35 2002

The structure and chemistry of 94 m Greenland Ice Sheet Project 2 ice

Ian BAKER, Daniel CULLEN
Thayer School of Engineering, Dartmouth College, Hanover, NH 03755-8000, U.S.A.
E-mail: ian.baker@dartmouth.edu

ABSTRACT. Optical microscopy, X-ray topography, scanning electron microscopy and X-ray spectroscopy have been used for microstructural analysis of ice from 94 m depth from Greenland Ice Sheet Project 2. The ice had a high density of air bubbles, a 2 mm grain-size and contained a high dislocation density in most grains ($>1 \times 10^{10}$ m^{-2}), although a few lower-dislocation-density grains were present. The main impurities, Na and Cl, were found in several grain boundaries and triple points, often as filaments. Na and Cl were also found in the lattice, but to a lesser extent, along with S, Mg, K and Ca. These observations are compared to previous studies of dislocations and impurity locations in natural ice.

INTRODUCTION

The spatial distribution of impurities in glacier ice has been a matter of interest and speculation for over a century (Buchanan, 1887). Even though concentrations of impurities in natural ice are quite low (Mayewski and others, 1993), their concentrations in grain boundaries, in water veins running along the grain triple junctions, and in the nodes where veins meet could be quite high (Nye and Frank, 1973; Harrison and Raymond, 1976; Maccagnan, 1981; Wolff and Paren, 1984). The microstructural locations of impurities in ice are important because they can have significant impacts on its electrical conduction, diffusion and mechanical properties.

There have been only two studies on the microchemistry of grain boundaries in glacier ice. The first, by Wolff and coworkers (Mulvaney and others, 1988; Wolff and others, 1988), used energy-dispersive spectroscopy (EDS) in a scanning electron microscope (SEM) to study ice from Dolleman Island, Antarctica, which was held at 113 K and aluminum-coated to prevent charging. They found substantial concentrations of sulfur at the triple junctions, but no impurities were detected at the grain boundaries. Neither Na nor Cl was detected even though ion chromatography showed they were present in the ice. In the second study, Fukazawa and others (1998) used microRaman spectroscopy to study triple junctions in ice from two Antarctic sites (Nansen and South Yamato). An advantage of Raman spectroscopy is that it detects chemical species rather than just elements (as in EDS). In the Nansen ice, NO_3^- and HSO_4^- were found as liquids at a triple junction at temperatures of 265–238 K. In the South Yamato ice, SO_4^{2-} was found as a liquid at the triple junctions at 265–253 K. It was estimated that all the nitric acid and sulfuric acid were located at the triple junctions in the Nansen ice, but that $<3\%$ of the sulfuric acid in the South Yamato ice was located at the triple junctions.

The density and distribution of dislocations also affect the electrical conduction, diffusion and mechanical properties of ice. For over three decades X-ray topography has been used to study dislocations in ice (Hayes and Webb, 1965). Topographs of glacier ice were first obtained from near-surface ice from Mendenhall Glacier, near Juneau, Alaska, U.S.A., and from ice from 2000 m at Byrd Station, Antarctica (Fukuda and Shoji, 1988).

Here, we attempt to present a complete characterization of the microstructure and microchemistry of naturally occurring ice from a single depth at Greenland Ice Sheet Project 2 (GISP2), using a combination of polarized-light optical microscopy, white-beam synchrotron X-ray topography, scanning electron microscopy and X-ray spectroscopy.

EXPERIMENTAL

The ice studied was from 94 m depth from the GISP2 site and was ~290 years old at the date of extraction (1989). Table 1 shows the chemistry of ice covering approximately a 2 year period, from which our ice was taken. There was little volcanic activity during this time period. The ice core, which was stored at 253 K at the National Ice Core Laboratory, Boulder, CO, U.S.A., was cut into three sections and examined optically, by X-ray topography and using a SEM/EDS system. For optical examination, a thin section of the ice was examined under cross-polarized sheets.

For X-ray topography, a razor blade was used to slowly slice off thin layers of the ice held at 263 K until the final specimen dimensions of 24 mm × 11 mm × 2 mm thick were obtained. Topographs were obtained by irradiating the ice,

Table 1. Impurities (ppb) in the ice cores from 94 m (93.44–93.92 m) at GISP2 (Mayewski and others, 1997; NSIDC, 1997) and 65 m at Dolleman Island (Wolff and others, 1988)

Site	*Na*	*NH_4*	K	*Mg*	*Ca*	*Cl*	*NO_3*	SO_4
94 m, GISP2	4.1	5.2	2.2	1.4	7.6	11	72	73
65 m, Dolleman Island	182	–	–	–	–	320	41	764

https://doi.org/10.3189/172756402781816627 Published online by Cambridge University Press

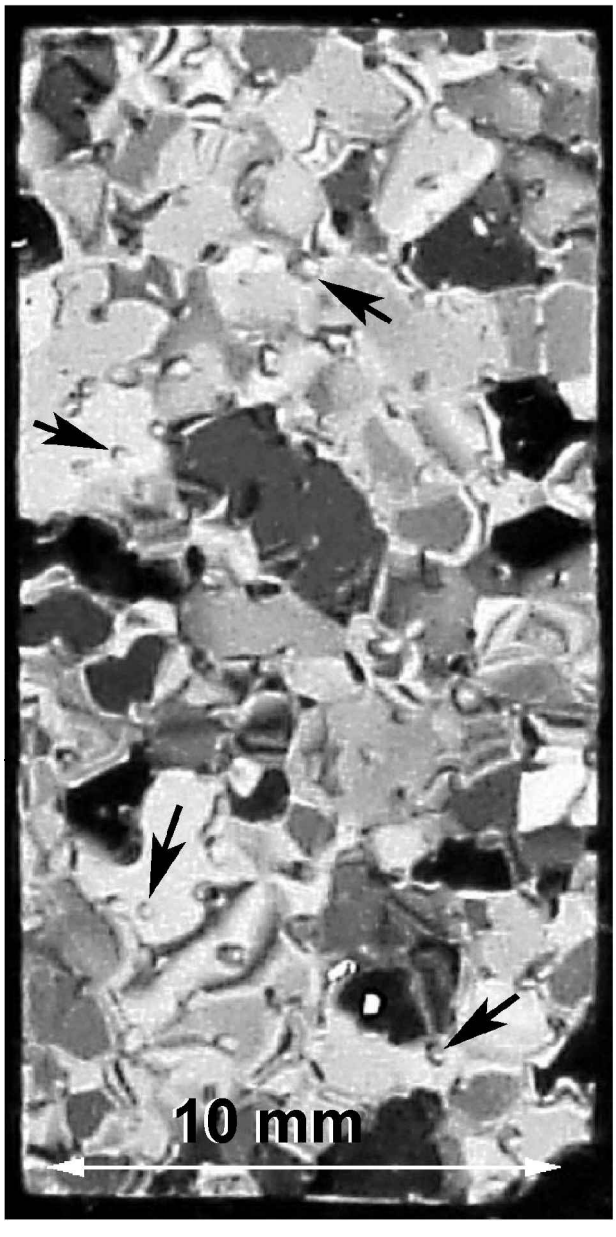

Fig. 1. Optical micrograph of thin section of ice. The arrows point to some of the many bubbles present.

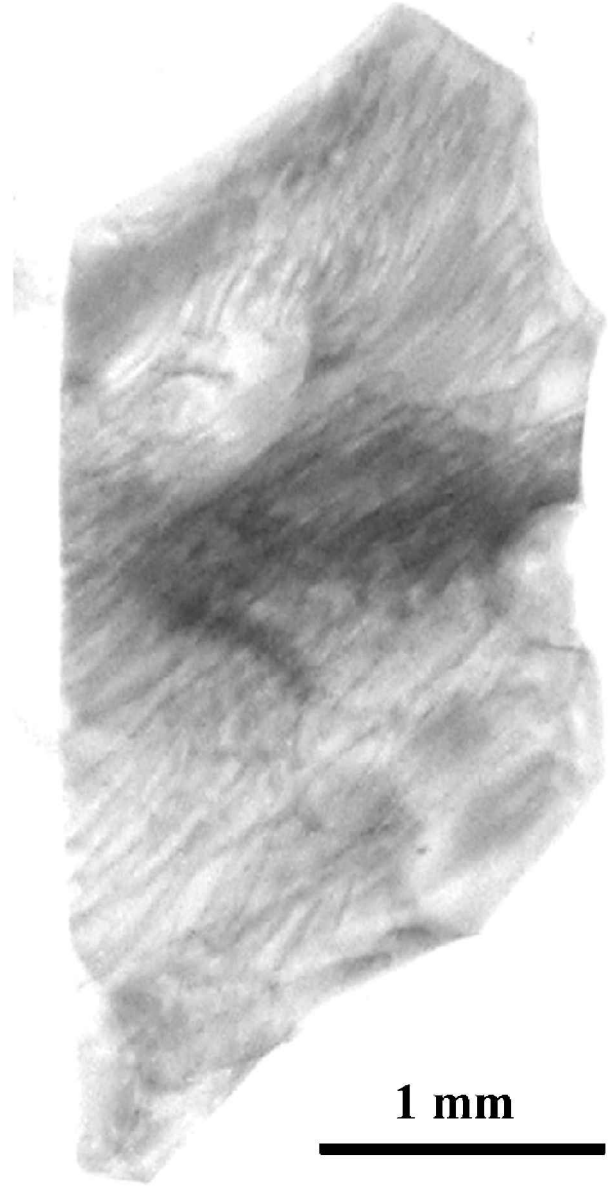

Fig. 2. X-ray topograph of a grain taken perpendicular to the ice-core axis. The dark "lines" within the grain are dislocations.

held at 263 K in a cryostat, with a highly collimated beam of white X-rays at the National Synchrotron Light Source (NSLS), Brookhaven National Laboratory, NY, U.S.A. Diffraction spots from several grains were recorded simultaneously in a single exposure of ~2–8 s. Each diffraction spot contains a two-dimensional image of the three-dimensional defect structure in a grain. Further details of the technique can be found elsewhere (Liu and others, 1992; Baker and Liu, 1994).

For examination in the SEM, ~25 mm × 25 mm × 10 mm thick specimens were cut, shaved flat with a razor blade under a High Efficiency Particle Air (HEPA)-filtered, laminar-flow hood at 253 K, and frozen onto a brass plate. The specimen was then either sealed in a small container for examination later or mounted onto a cold stage for immediate observation. The uncoated specimens were examined at 158 ±5 K using a Japanese Electron Optics Limited 5310 low-vacuum SEM, equipped with a Princeton Gamma Tech. IMIX EDS system utilizing a pure germanium, aluminum-coated polyimide thin-window detector, operated at 10 kV. Secondary electron (SE) imaging was used.

RESULTS AND DISCUSSION

Figure 1 is an optical micrograph of the ice observed under cross-polarizers. The grains, which have random *c*-axis orientations, have a 2 mm average grain-size and 4.7% porosity in the form of numerous small (~0.25 mm diameter) spherical bubbles (Gow and others, 1997).

X-ray topographic images of most grains were severely distorted with such a high dislocation density ($>1\times10^{10}$ m^{-2}) that individual dislocations could not be resolved. The exception was a few small grains where the dislocation density was $\sim1\times10^{7}$ m^{-2} (see Fig. 2). By comparison, dislocation densities found in ice samples from Mendenhall Glacier were much higher at 1×10^{8}–1×10^{9} m^{-2}, whereas ice from Byrd Station contained a mosaic structure but few dislocations (Fukuda and Shoji, 1988). It is likely that the small grains had dynamically recrystallized to a low dislocation density and subsequently undergone further deformation. Similar small grains containing a lower dislocation density than the surrounding material have been

https://doi.org/10.3189/172756402781816627 Published online by Cambridge University Press

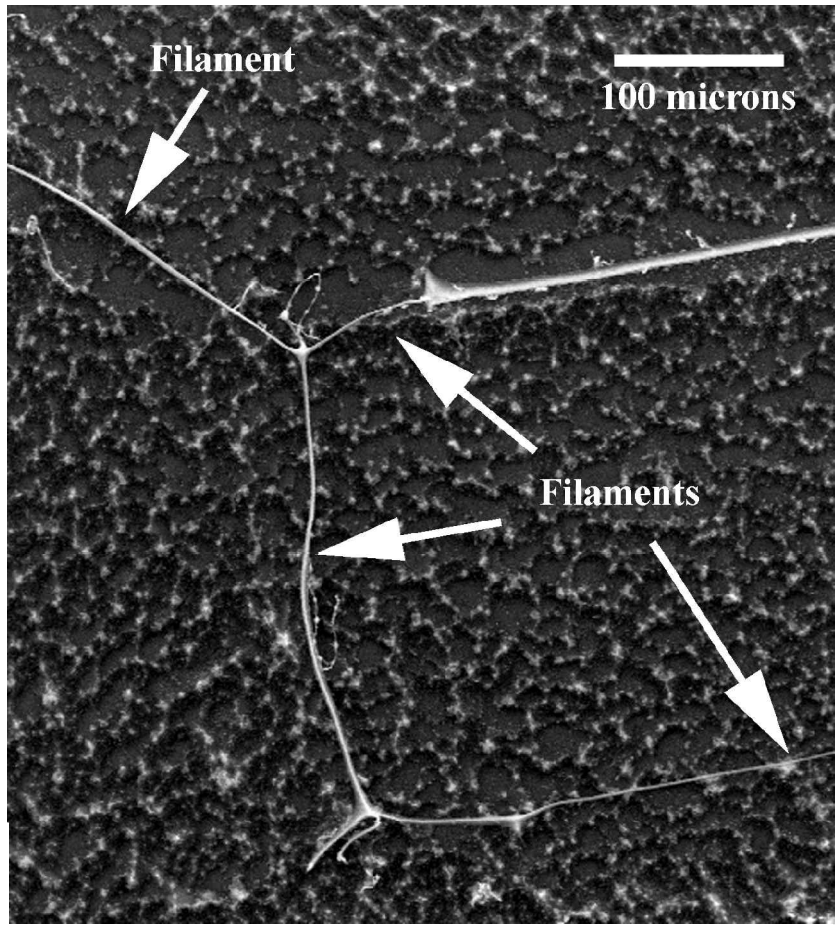

Fig. 3. SE image of ice allowed to sublimate for 6 weeks at 253 K, showing "filaments" (arrowed) along the grain boundaries that meet at "nodes". The upper "node" is shown at higher magnification in Figure 4.

observed by transmission electron microscopy in metallic materials that have dynamically recrystallized (Baker and others, 1984; Baker and Gaydosh, 1987).

Figure 3 is a SE image of ice that has been allowed to sublimate for 6 weeks at 253 K. Filaments are present along the grain boundaries and join together at triple junctions. The filaments are thought to form as a result of the coalescing of impurities that remain in the boundary plane after sublimation of the ice (Cullen and Baker, 2000).

Figure 4 shows higher-magnification images of the upper filament intersection in Figure 3, revealing what appear to be veins intersecting at nodes. It is not wholly clear whether these are veins or simply grain intersections with the surface. Near its melting point, ice contains water veins, which run along the grain triple junctions and meet at four-grain intersections or nodes (Steinemann, 1957; Ketcham and Hobbs, 1969; Paren and Walker, 1971; Nye and Mae, 1972; Nye and Frank, 1973; Raymond and Harrison, 1975; Nye, 1989, 1991; Mader, 1992a). Impurities increase the size of veins and depress their freezing points (Mader, 1992b). In so doing, impurities could dramatically increase diffusion rates (Nye, 1989) and produce highly conducting veins in a poorly conducting matrix, thus explaining the electrical behavior of Antarctic ice (Wolff and Paren, 1984).

X-ray spectra from the node's center show only Na and Cl (see Fig. 4b). (A spectrum from the other node gave an identical result.) Impurity elements typically found in glacier ice (Mayewski and others, 1993) are indicated on the X-ray spectra along with oxygen, which arises from the ice and/or hydrated impurities. Only Na and Cl are clearly present in these spectra. The small, unlabelled peak to the right of the large Cl (K_α) peak is its K_β peak. Na and Cl are usually found together and arise from sea-salt aerosols, but Cl can also occur independently of Na from HCl in the atmosphere. S can be introduced from sea salt (Na_2SO_4), continental dust ($CaSO_4$), and acidic compounds derived from marine biological sources (H_2SO_4 and CH_3SO_3H); and Mg, Ca and K arise from continental dust (Mayewski and others, 1997). Nitrogen, which is present in ice as NO_3^- and NH_4^+, is not indicated since at low concentrations we have found it to be undetectable using the present set-up. The ratio of the area under the Cl peak to that under the Na peak (which is related to the concentrations of the elements present) in Figure 4b is close to those we have obtained in spectra from NaCl crystals and frozen brine. Figure 4c shows X-ray maps for Na and Cl: Na and Cl are both clearly strongly associated with the veins and nodes and very little with the surrounding lattice.

Figure 5a shows ice that has been allowed to sublimate for 8 weeks at 253 K. The surface of the ice develops facets, which reflect the orientations of the grains, as noted previously (Cross, 1969; Cullen and Baker, 2000). The grain boundary and triple junction can be observed because of the different sublimation patterns of adjacent grains. The apexes of facets normally have a white spot associated with them. X-ray spectra from these white spots (labeled 1, 2 and 4 in Fig. 5a) almost invariably show the presence of impurities (in these spectra, just Na and Cl), whereas spectra from dark areas, whether in the grain boundary (spectrum 3) or the lattice, do not (see Fig. 5b).

The inset in Figure 6a shows ice that has been allowed to sublimate for 2 hours at 158 K in the SEM in which a filament

https://doi.org/10.3189/172756402781816627 Published online by Cambridge University Press

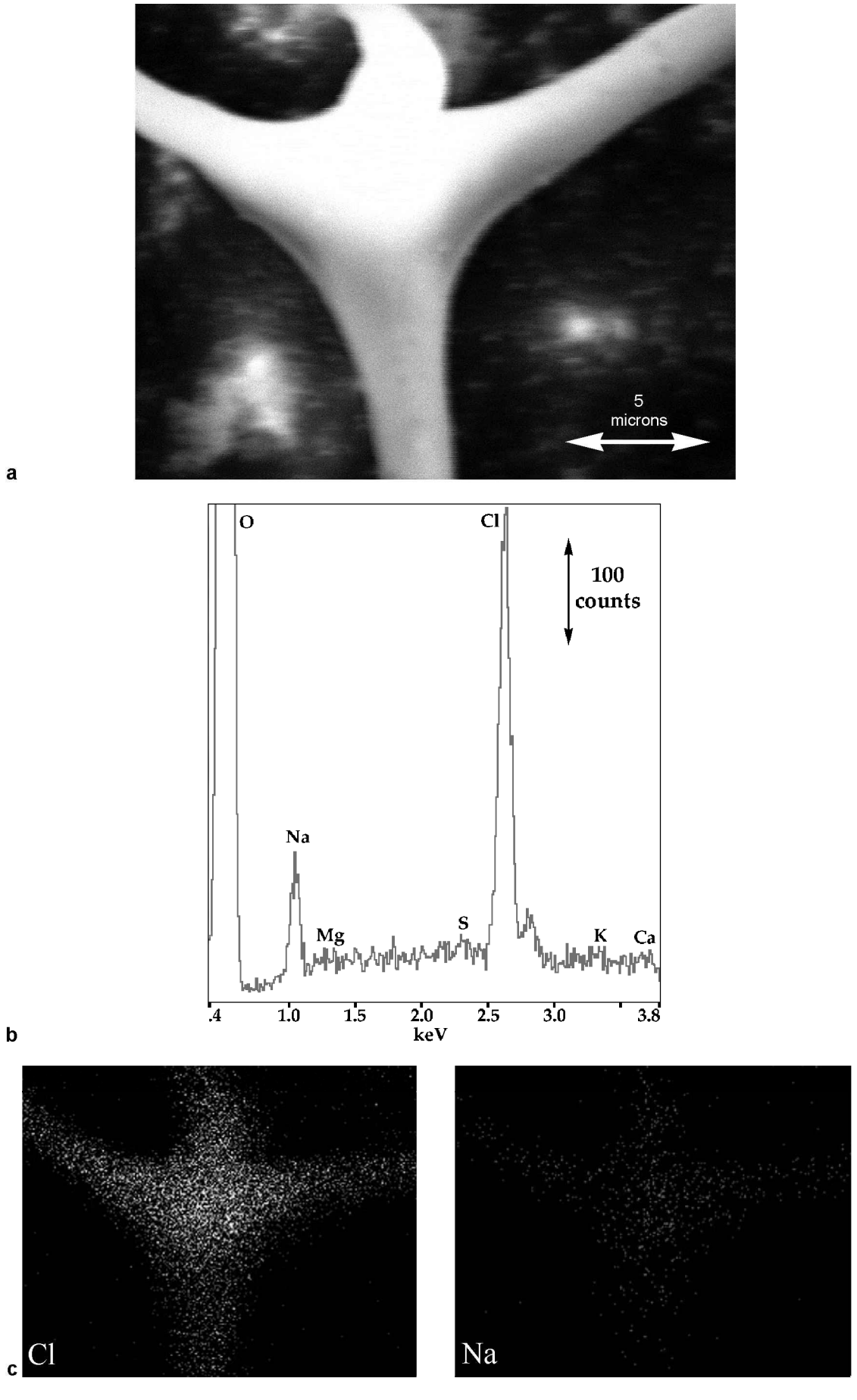

Fig. 4. (a) SE image of the upper "node" in Figure 3; (b) X-ray spectrum from the "node"; and (c) corresponding X-ray maps showing the distribution of Na and Cl.

https://doi.org/10.3189/172756402781816627 Published online by Cambridge University Press

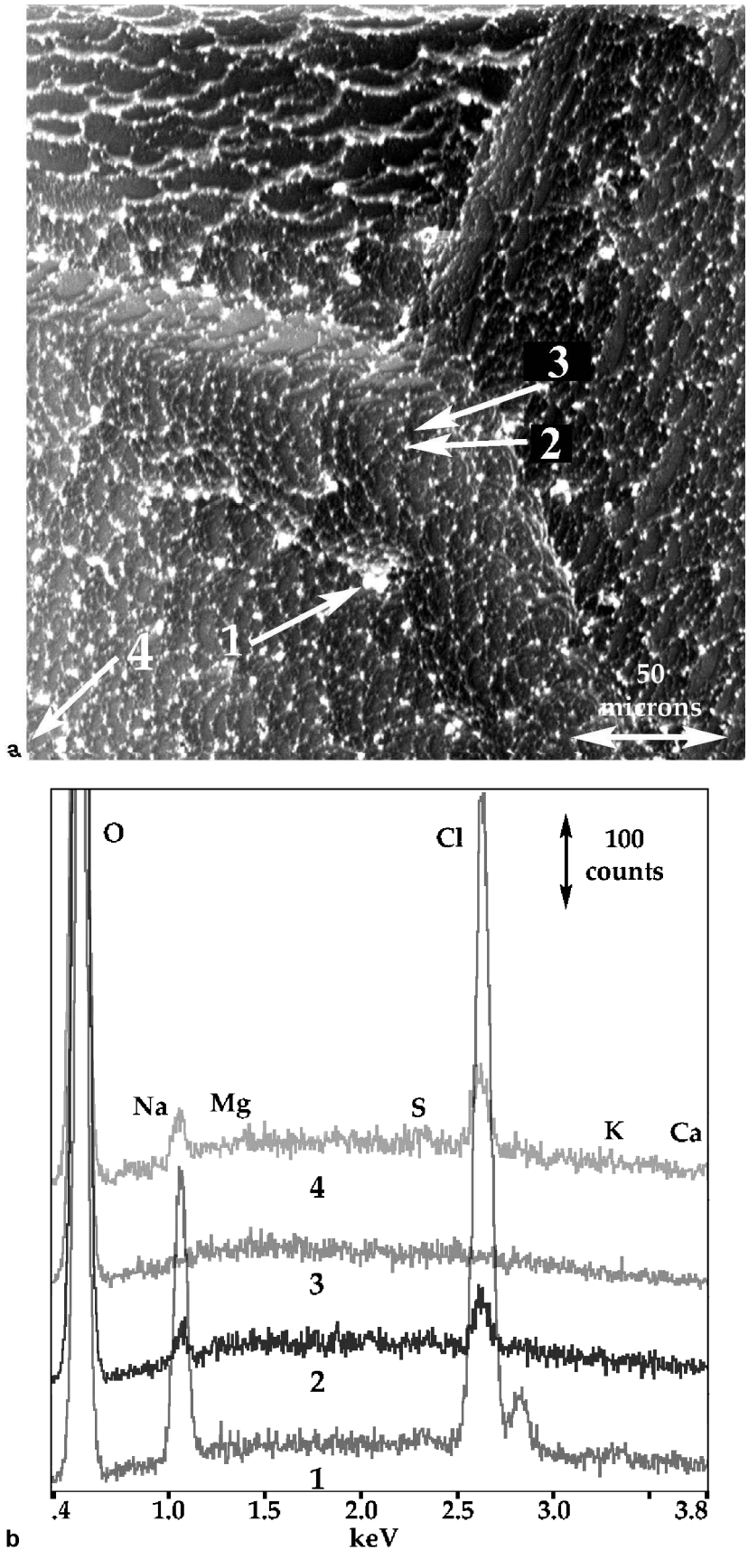

Fig. 5. (a) SE image of three grain boundaries and a triple junction in ice allowed to sublimate for 8 weeks at 253 K; and (b) X-ray spectra from the points indicated in (a). Point 1 is a white spot on the edge of the grain boundary; points 2 and 3 are white and black regions, respectively, in the triple junction; and point 4 is a white spot within the grain.

is present in the grain boundary (the boundary was more clearly visible optically). During observation the filament broke, and the result is shown in the larger image in Figure 6a. Filaments often moved during observation, probably due to both differential heating and charging from the electron beam. Spectra from this filament again showed mostly Na and Cl, but Mg, S, K and Ca are also present, particularly in the bulbous part, which presumably came from a triple junction or node (see Fig. 6b).

The observation that Na and Cl are the main impurities

https://doi.org/10.3189/172756402781816627 Published online by Cambridge University Press

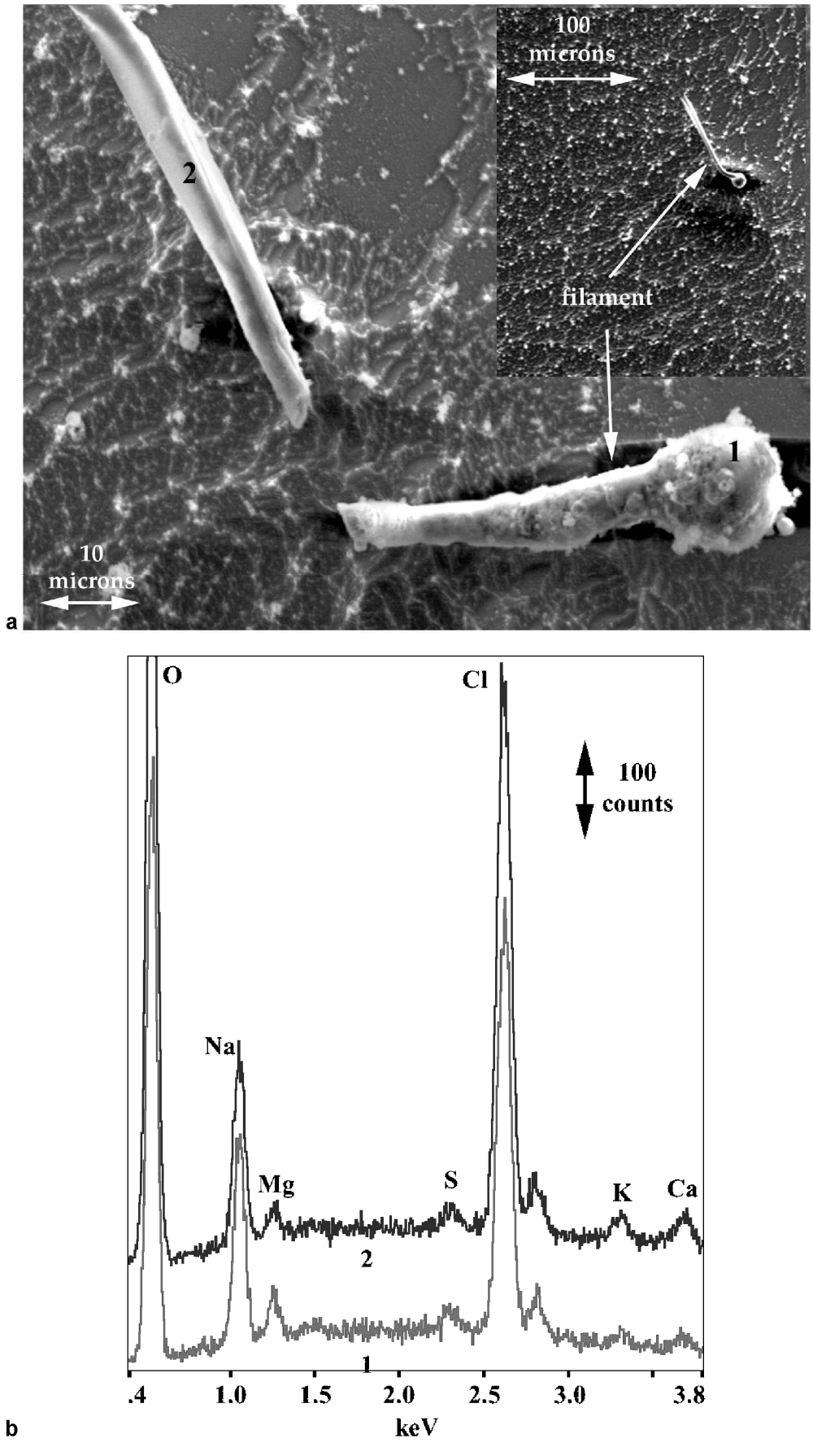

Fig. 6. (a) SE image of broken filament from a grain boundary, including inset showing the grain boundary where the filament originated, in ice allowed to sublimate for 2 hours at 158 K; and (b) X-ray spectra from the points on the filament indicated in (a).

in the grain boundaries in the ice from GISP2 at 94 m depth is different from the S observed in three triple junctions in 65 m ice (~125 years old) from Dolleman Island by Wolff and co-workers (Mulvaney and others, 1988; Wolff and others, 1988), or the sulfate or nitrate ions noted in triple junctions in ice from two Antarctic sites by Fukazawa and others (1998). Other work by the authors has shown that S appears to be common in the grain boundaries and lattice of ice from the GISP2 site (Cullen and Baker, 2000) and from Byrd Station (Cullen and Baker, in press). The

https://doi.org/10.3189/172756402781816627 Published online by Cambridge University Press

occurrence of other impurities (e.g. Mg, K, Ca) is less common and appears to be happenstance in the GISP2 ice.

The reasons for the differences observed in the microstructural locations of impurities, determined using SEM/EDS, between the GISP2 ice and the Dolleman Island ice are not wholly clear. The much higher (10 times) concentration of SO_4 at the Dolleman Island site (see Table 1), reflecting summer precipitation close to the open-water Weddell Sea, may be the reason S was observed to be highly concentrated in the triple junctions of that ice and not in the GISP2 ice. The difference in the mean temperatures between the two sites (241 K at GISP2; 256 K at Dolleman Island) may also play a small role, by allowing easier diffusion of the sulfate. However, differences in technique probably play a large role in explaining the other differences in the *observed* location of impurities. Wolff and others (1988) noted that their experimental procedure, which involved aluminum-coating the ice and keeping it at 113 K (with probably little sublimation of the ice occurring during examination), did not allow any decision to be made on whether acids (or, presumably, other species) were present on the grain boundaries (or, presumably, in the lattice). The technique used here allowed impurities to be observed in both these locations because the ice was uncoated and the impurities were concentrated by removing the ice through controlled sublimation. The suggestion by Mulvaney and others (1988) that it is thermodynamically preferable for NaCl in polar ice to partition to the grain boundaries appears to be borne out by our data (small Na and Cl concentrations in the grain interiors, but large concentrations in the form of filaments in the grain boundary) and calculations (Cullen and Baker, 2000, in press).

CONCLUSIONS

Ice from 94 m depth at the GISP2 site has been characterized using optical microscopy, X-ray topography, scanning electron microscopy and X-ray spectroscopy. The ice had a grain-size of ~ 2 mm and a high density of air bubbles. Most grains contained a high dislocation density ($>1 \times 10^{10}$ m^{-2}), although a few grains were present with a lower density. Na and Cl were present in many grain boundaries and triple points, and in the lattice to a lesser extent. S, Mg, K and Ca were also occasionally detected.

ACKNOWLEDGEMENTS

This research was supported by U.S. National Science Foundation grant OPP-9980379 and Army Research Office (ARO) grant DAAD 19-00-1-0444. The ARO provided funds for the SEM/EDS through grants DAAH 04-96-1-0292 and DAAD 19-99-10068. We would like to thank A. J. Gow of the U.S. Army Cold Regions Research and Engineering Laboratory, Hanover, NH, for the GISP2 specimen, and M. Dudley of the State University of New York, Stony Brook, NY, for use of beam line X19C at NSLS.

REFERENCES

Baker, I. and D. J. Gaydosh. 1987. Dynamic recrystallization and grain boundary migration in B2 FeAl. *Metallography*, **20**, 347–357.

Baker, I. and F. Liu. 1994. On *in-situ* study of dislocation/grain boundary interactions using X-ray topography and TEM. *Mater. Res. Soc. Symp. Proc.*, **319**, 203–214.

Baker, I., D. V. Viens and E. M. Schulson. 1984. Metallographic observations of dynamic recrystallization in Ni_3Al. *Scripta Metall.*, **18**, 237–240.

Buchanan, J. Y. 1887. On ice and brines. *Proc. R. Soc. Edinburgh*, **14**, 129–149.

Cross, J. D. 1969. Scanning electron microscopy of evaporating ice. *Science*, **164**(3876), 174–175.

Cullen, D. and I. Baker. 2000. Correspondence. The chemistry of grain boundaries in Greenland ice. *J. Glaciol.*, **46**(155), 703–706.

Cullen, D. and I. Baker. In press. Observation of impurities in ice. *Microscopy Res. Techn.*

Fukazawa, H., K. Sugiyama, S. Mae, H. Narita and T. Hondoh. 1998. Acid ions at triple junction of Antarctic ice observed by Raman scattering. *Geophys. Res. Lett.*, **25**(15), 2845–2848.

Fukuda, A. and H. Shoji. 1988. Dislocations in natural ice crystals. *In* Higashi, A., *ed. Lattice defects in ice crystals; X-ray topographic observations.* Sapporo, Hokkaido University Press, 13–25.

Gow, A. J. *and 6 others*. 1997. Physical and structural properties of the Greenland Ice Sheet Project 2 ice cores: a review. *J. Geophys. Res.*, **102**(C12), 26,559–26,575.

Harrison, W. D. and C. F. Raymond. 1976. Impurities and their distribution in temperate glacier ice. *J. Glaciol.*, **16**(74), 173–181.

Hayes, C. E. and W. W. Webb. 1965. Dislocations in ice. *Science*, **147**(3653), 44–45.

Ketcham, W. M. and P. V. Hobbs. 1969. An experimental determination of the surface energies of ice. *Philos. Mag.*, **19**(162), 1161–1173.

Liu, F., I. Baker, G. Yao and M. Dudley. 1992. Dislocations and grain boundaries in polycrystalline ice: a preliminary study by synchrotron X-ray topography. *J. Mater. Sci.*, **27**(10), 2719–2725.

Maccagnan, M. 1981. Contribution à l'étude des propriétés diélectriques de la glace Antarctique, application géochimique. (Thèse de 3ième cycle, Grenoble, Laboratoire de Glaciologie du CNRS et Université Joseph Fourier.) (Publ. 373.)

Mader, H. M. 1992a. Observations of the water-vein system in polycrystalline ice. *J. Glaciol.*, **38**(130), 333–347.

Mader, H. M. 1992b. The thermal behaviour of the water-vein system in polycrystalline ice. *J. Glaciol.*, **38**(130), 359–374.

Mayewski, P. A. *and 7 others*. 1993. The atmosphere during the Younger Dryas. *Science*, **261**(5118), 195–197.

Mayewski, P. A. *and 6 others*. 1997. Major features and forcing of high-latitude Northern Hemisphere atmospheric circulation using a 110,000 year-long glaciochemical series. *J. Geophys. Res.*, **102**(C12), 26,345–26,366.

Mulvaney, R., E. W. Wolff and K. Oates. 1988. Sulphuric acid at grain boundaries in Antarctic ice. *Nature*, **331**(6153), 247–249.

National Snow and Ice Data Center (NSIDC). 1997. *The Greenland Summit ice cores.* Boulder, CO, University of Colorado. Cooperative Institute for Research in Environmental Sciences. National Snow and Ice Data Center, Distributed Active Archive Center.

Nye, J. F. 1989. The geometry of water veins and nodes in polycrystalline ice. *J. Glaciol.*, **35**(119), 17–22.

Nye, J. F. 1991. Thermal behaviour of glacier and laboratory ice. *J. Glaciol.*, **37**(127), 401–413.

Nye, J. F. and F. C. Frank. 1973. Hydrology of the intergranular veins in a temperate glacier. *International Association of Scientific Hydrology Publication* 95 (Symposium at Cambridge 1969 — *Hydrology of Glaciers*), 157–161.

Nye, J. F. and S. Mae. 1972. The effect of non-hydrostatic stress on intergranular water veins and lenses in ice. *J. Glaciol.*, **11**(61), 81–101.

Paren, J. G. and J. C. F. Walker. 1971. Influence of limited solubility on the electrical and mechanical properties of ice. *Nature*, **230**(12), 77–79.

Raymond, C. F. and W. D. Harrison. 1975. Some observations on the behavior of the liquid and gas phases in temperate glacier ice. *J. Glaciol.*, **14**(71), 213–233.

Steinemann, A. 1957. Dielektrische Eigenschaften von Eiskristallen II. Teil Dielektrische Untersuchungen an Eiskristallen mit Eingelagerten Fremdatomen. *Helv. Phys. Acta*, **30**, 553–610.

Wolff, E. W. and J. G. Paren. 1984. A two-phase model of electrical conduction in polar ice sheets. *J. Geophys. Res.*, **89**(B11), 9433–9438.

Wolff, E. W., R. Mulvaney and K. Oates. 1988. The location of impurities in Antarctic ice. *Ann. Glaciol.*, **11**, 194–197.